EUROPEAN ORGANIZATION FOR NUCLEAR RESEARCH

L3 Note 2750
June 26, 2002

# Inclusive Charged Hadron Production in Two-Photon Collisions at LEP

The L3 Collaboration

## Abstract

The reaction $e^+e^- \rightarrow e^+e^-\ h^\pm\ X$ is studied using data collected at LEP with the L3 detector at centre-of-mass energies between 189 and 202 GeV. The inclusive charged hadron production is analysed, as well as the pion and kaon contributions. Differential cross sections - for charged particles production - are measured as a function of the particle transverse momentum $p_t$. For $p_t \leq 1.5$ GeV, the differential cross sections are described by an exponential, typical of soft hadronic processes. For $p_t \geq 1.5$ GeV, the cross section shows the presence of perturbative QCD processes, described by a power-law. The data are compared to Monte Carlo predictions. The $K^\pm$ production is in good agreement with the previous inclusive $K^0_S$ measurement. The $\pi^\pm$ production is in good agreement with the previous inclusive $\pi^0$ measurement and is compared to NLO QCD prediction. For inclusive $\pi^\pm$, the differential cross section is also measured as a function of the pseudo-rapidity. All the results are preliminary.

Submitted to the $31^{st}$ *International Conference on High Energy Physics*
Amsterdam, Netherlands, 24-31 July 2002.

# 1 Introduction

Two-photon collisions are the main source of hadron production in the high-energy regime of LEP via the process $\mathrm{e^+e^-} \rightarrow \mathrm{e^+e^-}\gamma^*\gamma^* \rightarrow \mathrm{e^+e^-}\mathit{hadrons}$. In the Vector Dominance Model, each photon can transform into a vector meson with the same quantum numbers, thus initiating a strong interaction process with characteristics similar to hadron-hadron interactions. This process dominates in the "soft" interaction region, where hadrons are produced with a low transverse momentum $p_t$. Hadrons with high $p_t$ are produced by the direct QED process $\gamma^*\gamma^* \rightarrow \mathrm{q\bar{q}}$ or by QCD processes originating from the partonic content of the photon. QCD calculations are available for single particle inclusive production in two-photon interactions at next-to-leading order (NLO) [1, 2].

The process $\mathrm{e^+e^-} \rightarrow \mathrm{e^+e^-}\mathit{hadrons}$ is modelled with the PHOJET [6] and PYTHIA [7] event generators with respectively 2 and 3 times more luminosity than the data. The lack of generated hadrons at high $p_t$ with the generator PHOJET doesn't allow us to use this generator for efficiency calculation. In this study, it will only be used in the final comparison with the experimental cross section. For the PHOJET generator, 4 classes of $\gamma\gamma$ events are taken into account : the VDM, where each photon interacts as a vector meson, the direct $\gamma^*\gamma^* \rightarrow \mathrm{q\bar{q}}$ process, the single resolved and the double resolved processes, where respectively 1 or 2 photons are interacting through its partonic content. For the PYTHIA generator, each photon can interact as a pointlike particle, as a vector meson or as a resolved photon, leading to 6 classes of events. Another difference between the two generators is the treatment of soft interaction. In the PYTHIA model, a soft event consists always of one soft interaction: soft interactions are not generated for events having one or more hard interactions. In the PHOJET model, as it uses the Dual Parton Model [8], there are several soft and hard interactions within one event possible. In particular, a soft event is, in general, built up by several soft interactions. One has to keep in mind that the typical transverse momentum cutoff which separate soft and hard interactions is of the order of 0.5 GeV in PYTHIA whereas it is about 2.5-3 GeV in PHOJET [9]. Both generators use JETSET for the fragmentation.

Recently, L3 published an analysis of inclusive $\pi^0$ and $\mathrm{K^0_S}$ production from quasi-real photons [3]. In the $\pi^0$ case, the differential cross section measured as a function of the particle transverse momentum $p_t$ exhibits a clear deviation from QCD calculations and Monte Carlo predictions. A comparison of these results with other single particle inclusive production at high $p_t$ is therefore important.

In this paper, inclusive charged hadron, $\pi^\pm$ and $\mathrm{K}^\pm$ productions from quasi-real photons are studied for a centre-of-mass energy of the two interacting photons, $\mathrm{W}_{\gamma\gamma}$, greater than 5 GeV. The hadrons are measured in the transverse momentum range $0.4 \leq p_t \leq 20$ GeV and in the pseudo-rapidity[1)] interval $|\eta| \leq 1$. All the results are preliminary.

The data used for this analysis were collected by the L3 detector [4] at centre-of-mass energies from $\sqrt{s} = 189$ GeV to 202 GeV, with a luminosity weighted average value of $\sqrt{s} = 194$ GeV. The integrated luminosity is 414 $\mathrm{pb^{-1}}$. Previous measurements of inclusive charged hadron production were performed at LEP [5] at $\sqrt{s} = 161 - 172$ GeV.

The following generators are used to simulate background processes: KK2f [10] for $\mathrm{e^+e^-}\rightarrow \mathrm{q\bar{q}}\,(\gamma)$; KORALZ [11] for $\mathrm{e^+e^-}\rightarrow \tau^+\tau^-(\gamma)$; KORALW [12] for $\mathrm{e^+e^-}\rightarrow \mathrm{W^+W^-} \rightarrow$ hadrons and DIAG36 [13] for $\mathrm{e^+e^-}\rightarrow \mathrm{e^+e^-}\tau^+\tau^-$. The events are simulated in the L3 detector using the GEANT [14] and GEISHA [15] programs and passed through the same reconstruction program as the data. Time dependent detector inefficiencies, as monitored during the data taking period,

[1)] $\eta = -\ln\ \tan(\theta/2)$, where $\theta$ is the polar angle of the particle relative to the beam axis.

are also simulated.

## 2 Event selection

The selection of $e^+e^- \to e^+e^- hadrons$ events [16] consists in:

- A multiplicity cut: to select hadronic final states, at least six objects must be detected. An object can be a track or a cluster in the calorimeters, with no associated track.
- Energy cuts: the total energy deposited in all the calorimeters must be smaller than 40 % of the centre of mass energy, in order to exclude annihilation events. The total energy in the electromagnetic calorimeter is required to be greater than 500 MeV, to suppress beam-gas and beam-wall backgrounds.
- An anti-tag condition: events with an electromagnetic shower shape, an energy greater than 30 GeV in a fiducial region of 33-64 mrad are excluded.

About 2 million hadronic events are selected. The level of background is less than 1% and is mainly due to the $e^+e^- \to q\bar{q}\,(\gamma)$ and $e^+e^- \to e^+e^-\tau^+\tau^-$ processes. The effective mass of all measured particles, $W_{\gamma\gamma}$, must be greater than 5 GeV. The mean value is $\langle W_{\gamma\gamma}\rangle \simeq 30$ GeV.

In the detector, charged hadron are seen as charged tracks in the inner tracking detector. Tracks must have a transverse momentum above 100 MeV and a distance of closest approach to the primary vertex in the transverse plane below 4 mm. The number of hits must be greater than 80% of that allowed by the track lenght. The tracks are analysed in the $|\eta| < 1$ range.

## 3 Charged hadrons differential cross section

The $p_t$ differential cross sections is measured for $W_{\gamma\gamma} \geq 5$ GeV, with a mean value of $\langle W_{\gamma\gamma}\rangle \simeq$ 30 GeV, and a photon virtuality $Q^2 \leq 8$ GeV$^2$, in 12 $p_t$ bins between 0.4 and 20 GeV.

The data are corrected for selection efficiency, including acceptance, calculated bin by bin with the Monte Carlo generator PYTHIA. The selection efficiency varies from 60 to 85%. The inefficiency at low $p_t$ is due to the effect of mass and energy cuts. The high $p_t$ inefficiency is dominated by the multiplicity cut since high $p_t$ particles are mainly produced in low multiplicity events.

Two-photon events are collected predominantly by the track triggers [18]. The trigger efficiency is obtained from each year's data sample by comparing the number of events accepted by the independent track and calorimetric energy [19] triggers. The efficiency of higher level triggers is 95 % and is measured using prescaled events.

The differential cross section of charged hadron production as a function of $p_t$ is shown in Figure 1. The background, subtracted bin by bin, remains very low over the whole $p_t$ range. $e^+e^- \to e^+e^-\tau^+\tau^-$ events dominate the background at low $p_t$ while annihilation events dominate it at high $p_t$. The level of background is shown on Figure 1a.

Sources of systematic uncertainties on the cross-section measurements are selection criteria, background subtraction and accuracy of the efficiencies estimate. The uncertainty due to selection criteria is evaluated varying cut criteria: the multiplicity cut is moved from 5 to 7 objects, the energy cut is moved to 35 % of $\sqrt{s}$ and the track number of hits is moved to 70 % of that allowed by the track lenght. Moving the other criteria give negligible contributions.

The uncertainty on the trigger efficiency and the uncertainty on the background subtraction are due to the statistical accuracy of their determination. To evaluate the uncertainty on the efficiency correction we calculate it by using only one of the PYTHIA subprocesses: VDM×VDM, direct×direct and resolved×resolved. The mean difference between them is used.

To check that the migration due to the $p_t$ resolution doesn't affect our analysis, an unfolding of the track $p_t$ distribution is also performed. The unfolding is done using one-step bayesian method [17]. The two methods are compatible within errors.

The steep decrease of $d\sigma/dp_t$ in the range $0.4 < p_t < 1.5$ GeV is described by an exponential of the form $Ae^{-p_t/\langle p_t \rangle}$ with a mean value of $\langle p_t \rangle \simeq 232$ MeV. This behaviour is characteristic of hadrons produced by soft interactions and is similar to that obtained in hadron-hadron and photon-hadron collisions [20]. For $p_t \geq 1.5$ GeV, the differential cross sections are better represented by a power law function $Ap_t^{-B}$, as expected by the onset of QCD processes. The value of the power B is 4. The fits are drawn on Figure 1a.

The differential cross sections are also compared to Monte Carlo predictions in Figure 1b. In the high $p_t$ region the two models are very different and are not reproducing the data. As already abserved [3] PYTHIA is slightly above the data, whereas PHOJET is too low by more than one order of magnitude.

# 4 Charged pion and charged kaon differential cross sections

From the charged hadron cross section, we extract the charged pion and the charged kaon inclusive cross sections. Their ratio relative to charged hadrons, called respectively pion purity and kaon purity, is calculated bin by bin with the Monte Carlo generator. The uncertainty on purities is calculated the same way as the uncertainty on efficiency: using different subprocesses of PYTHIA. It gives an additionnal uncertainty from 2 to 12% for pions and from 14 to 24% for kaons.

The differential cross section of $\pi^{\pm}$ production and of $K^{\pm}$ production as a function of $p_t$ are shown in Figure 2.

The $\pi^{\pm}$ data are compared to the previous $\pi^0$ data [3] scaled up by a factor 4: a factor 2 to correct for the $|\eta| < 0.5$ interval of the $\pi^0$ measurement and a factor 2 to take into account the isospin symmetry. A good agreement is found between these two measurements as shown in Figure 2a. The measured $\chi^2/d.o.f$, considering the systematic uncertainties to be uncorrelated, is 9.3 / 12. The $K^{\pm}$ data are compared to the previous results of $K^0_S$ data [3] scaled up by a factor 4/3: a factor 2/3 to correct for the $|\eta| < 1.5$ interval of the $K^0_S$ measurement and a factor 2 to take into account the isospin symmetry. A good agreement is found between these two measurements as shown in Figure 2b. The measured $\chi^2/d.o.f$, considering uncorrelated uncertainties, is 4.0 / 7. This is a good test of the fragmentation functions implemented in JETSET.

The differential cross section of $\pi^{\pm}$ production as a function of $|\eta|$ for $p_t > 1$ GeV is shown in Figure 3. The agreement with the previous measurement [3] is good. Monte Carlo and QCD predictions describe well the shape of the data. The absolute normalisation depends on the $p_t$ range considered.

In Figure 4a the data are compared to analytical NLO QCD predictions [2, 21]. For this calculation, the flux of quasi-real photons is obtained using the Equivalent Photon Approximation, taking into account both transverse and longitudinal virtual photons. The interacting particles can be photons or partons from the $\gamma \to q\bar{q}$, which evolve into quarks and gluons. The NLO parton density functions of Reference [22] are used and all elementary $2 \to 2$ and $2 \to 3$ processes are considered. New NLO fragmentation functions [23] are used. The renormalization, factorisation and fragmentation scales are taken to be equal: $\mu = M = M_F = \xi p_t$ [2]. The scale uncertainty in the NLO calculation is estimated by varying the value of $\xi$ from 0.5 to 2.0. The calculations, performed for $|\eta| < 0.5$, are scaled up by a factor 2 as the $d\sigma/d|\eta|$ cross section is flat. The agreement with the data is poor in the high-$p_t$ range. We have verified that the direct process simulated by PYTHIA gives the same cross section as the direct process predicted by the NLO calculation.

# References


[1] L. E. Gordon, Phys. Rev. **D 50** (1994) 6753.

[2] J. Binnewies, B. A. Kniehl and G. Kramer, Phys. Rev. **D 53** (1996) 6110.

[3] L3 Coll., P. Achard et al., Phys. Lett. **B 524** (2002) 44.

[4] L3 Coll., B. Adeva et al., Nucl. Instr. Meth. **A 289** (1990) 35; L3 Coll., M. Acciarri et al., Nucl. Instr. Meth. **A 351** (1994) 300.

[5] OPAL Coll., G. Abbiendi *et al.*, Eur. Phys. J. **C 6** (1999) 253.

[6] PHOJET version 1.05c is used with default options;
R. Engel, Z. Phys. **C 66** (1995) 203 ;
R. Engel and J. Ranft, Phys. Rev. **D 54** (1996) 4246;
R. Engel private communication.

[7] PYTHIA version 5.722 and JETSET version 7.409 are used with default options;
T. Sjöstrand, Comp. Phys. Comm. **82** (1994) 74.

[8] A. Capella et al., Phys. Rep. **236** (1994) 225.

[9] R. Engel, thesis, Siegen 1997.

[10] KK2f version 4.12 is used;
S. Jadach, B. F. L. Ward Z. Wąs, Comp. Phys. Comm. **130** (2000) 260.

[11] S. Jadach, B. F. L. Ward and Z. Wąs, Comp. Phys. Comm. **79** (1994) 503.

[12] M. Skrzypek, S. Jadach, W. Placzek, and Z. Wąs, Comp. Phys. Comm. **94** (1996) 216.

[13] F. A. Berends, P. H. Daverfeldt and R. Kleiss, Nucl. Phys. **B 253** (1985) 441.

[14] R. Brun et al., GEANT 3.15 preprint CERN DD/EE/84-1 (1984), revised 1987.

[15] H. Fesefeldt, RWTH Aachen report PITHA 85/2 (1985).

[16] L3 Coll., M. Acciarri *et al.*, Phys. Lett. **B 519** (2001) 33.

[17] G. D'Agostini, Nucl. Instr. Meth. **A 362** (1995) 487.

[18] P. Béné et al., Nucl. Instr. Meth. **A 306** (1991) 150;
D. Haas et al., Nucl. Instr. Meth. **A 420** (1999) 101.

[19] R. Bizzarri *et al.*, Nucl. Instr. Meth. **A 283** (1989) 799.

[20] M. L. Perl, *High Energy Hadron Physics* (ed. John Wiley, New-York, 1974).

[21] B. A. Kniehl, private communication.

[22] P. Aurenche, J.-P. Guillet, M. Fontannaz, Zeit. Phys. **C 64** (1994) 621.

[23] B. A. Kniehl, G. Kramer and B. Pötter, Nucl. Phys. **B 582** (2000) 514.

[24] J. Binnewies, B. A. Kniehl and G. Kramer, Phys. Rev. **D 52** (1995) 4947.

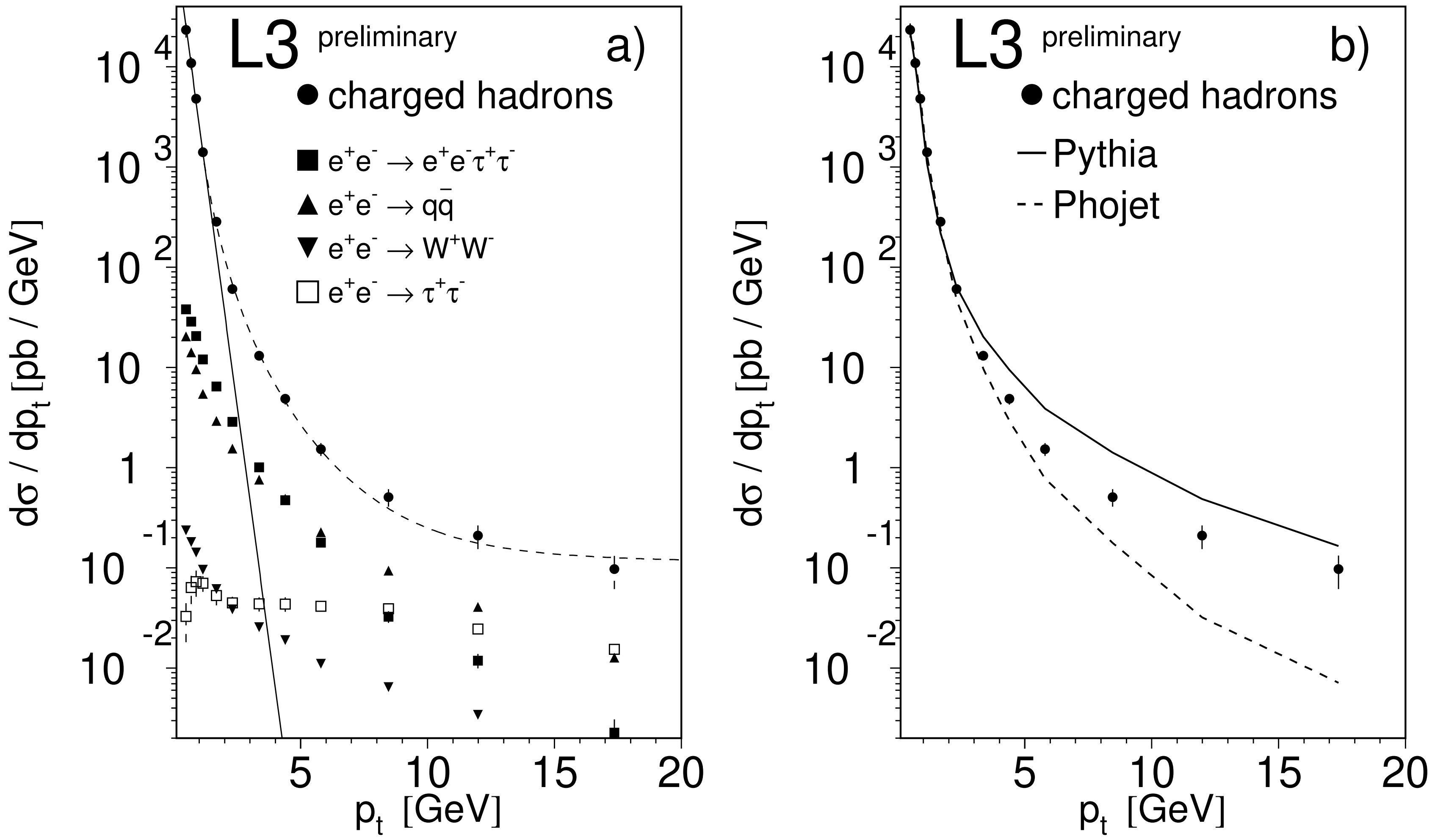


Figure 1: Inclusive charged hadrons differential cross section $d\sigma/dp_t$ a) fitted with an exponential (solid line) and a power-law function (dotted line) and b) compared with Monte-Carlo predictions. $\gamma\gamma \to \tau\tau$, $e^+e^- \to$ hadrons and $W^+W^- \to$ hadrons backgrounds, already subtracted from the cross section, are shown in a).

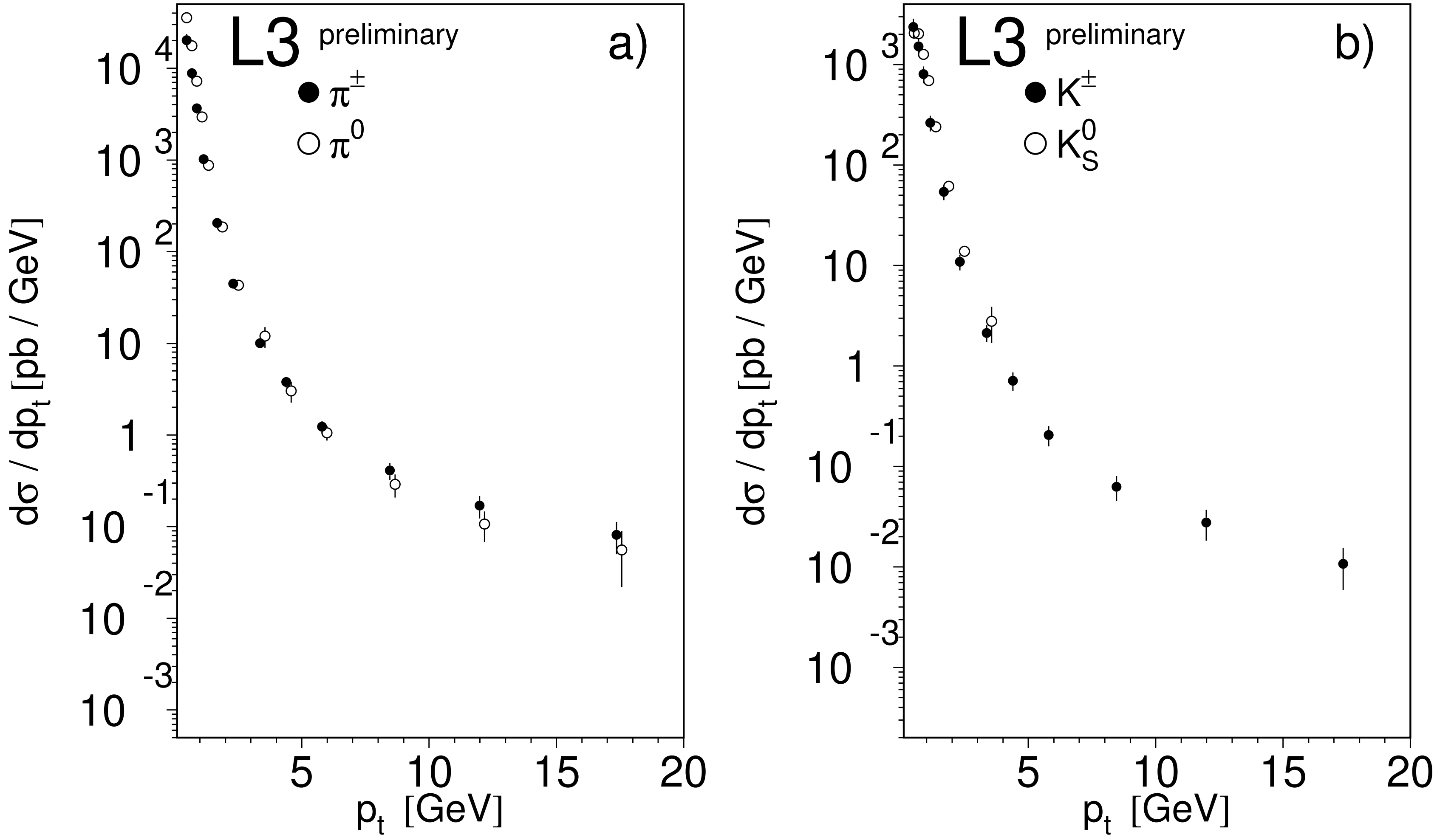


Figure 2: Differential cross section $d\sigma/dp_t$ for a) inclusive charged pion production and b) inclusive charged kaon production. The $\pi^{\pm}$ production is compared to the inclusive $\pi^0$ measurement scaled by a factor 4 (see text) and shifted by 200 MeV to avoid overlaping points. The $\mathrm{K}^{\pm}$ production is compared to the inclusive $\mathrm{K}^0_\mathrm{S}$ measurement scaled by a factor 4/3 (see text) and shifted by 200 MeV

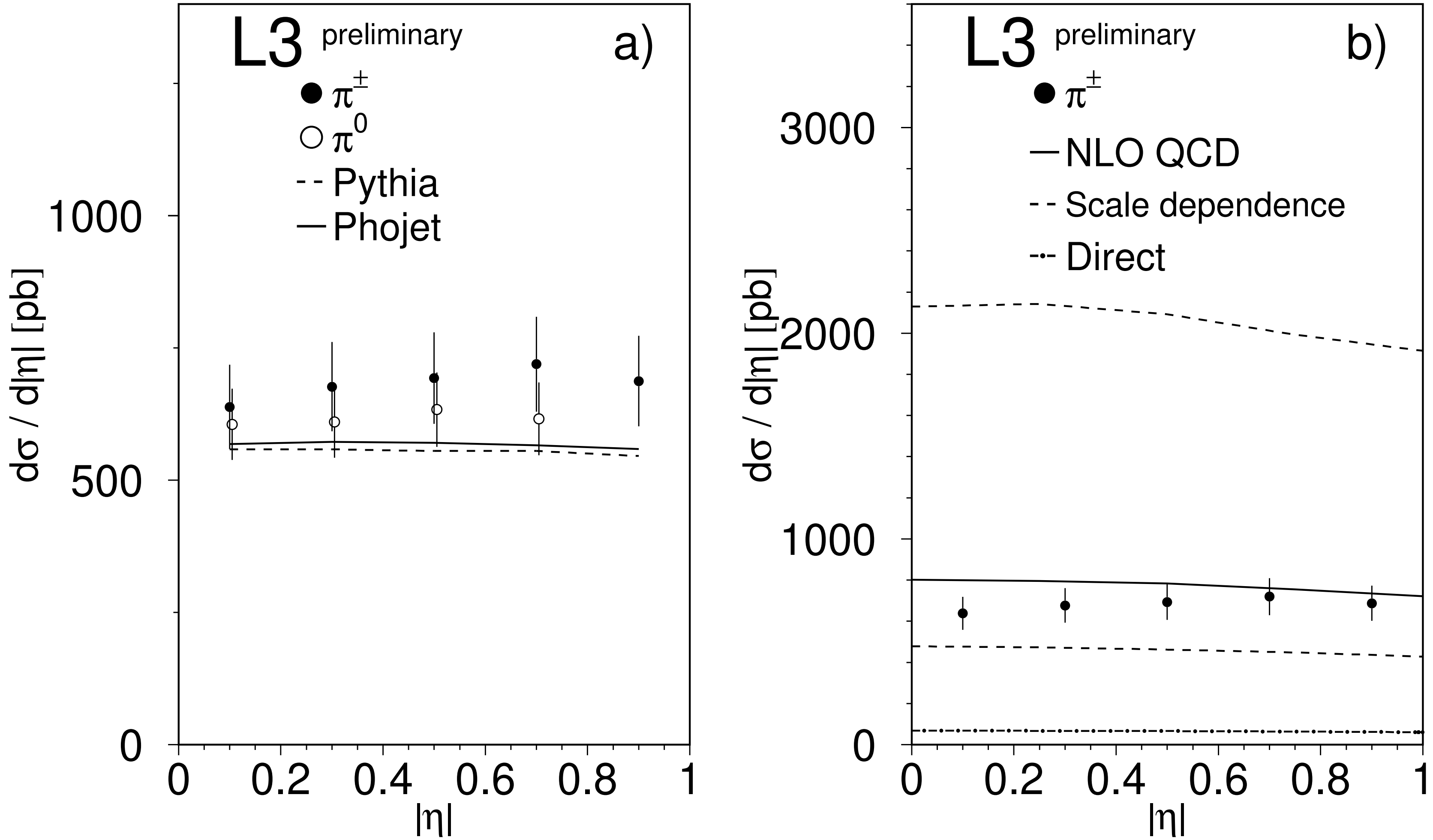


Figure 3: Inclusive $\pi^{\pm}$ differential cross section $d\sigma/d|\eta|$ compared to a) inclusive $\pi^0$ measurement and Monte Carlo predictions and b) NLO QCD calculation .

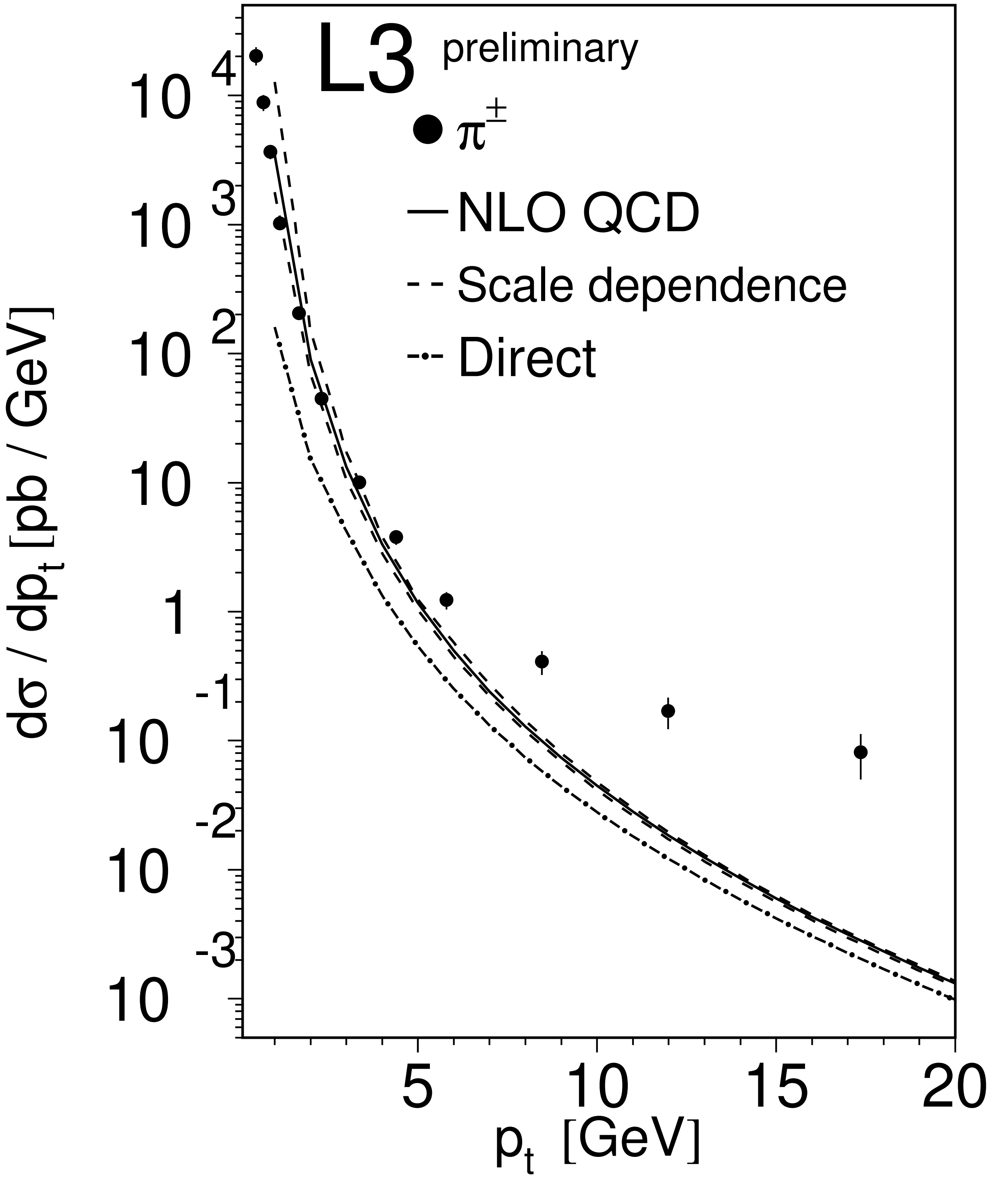


Figure 4: Inclusive $\pi^{\pm}$ differential cross section $d\sigma/dp_t$ compared to NLO QCD calculations. The dashed-dotted line correspond to the direct subprocess as calculated in the NLO QCD framework. The dashed lines are the scale uncertainty of calculations (see text).